

3. Blasse, G. *J. Appl. Phys.* **1965**, *36*, 879.
4. Omeran, I. *Thèse 3ème cycle*; Univ. Bordeaux I, **1976**, no. 1328.
5. Byeon, S. H.; Demazeau, G.; Fournès, L.; Dance, J. M.; Choy, J. H. *Solid State Comm.* **1991**, *80*, 457.
6. Demazeau, G.; Zhu, L. M.; Fournès, L.; Pouchard, M.; Hagenmuller, P. *J. Solid State Chem.* **1988**, *72*, 31.
7. Zhu, L. M.; Demazeau, G.; Pouchard, M.; Dance, J. M.; Hagenmuller, P. *J. Solid State Chem.* **1989**, *78*, 46.
8. Villeneuve, G.; Rojo, T.; Demazeau, G.; Hagenmuller, P. *Mat. Res. Bull.* **1988**, *23*, 1787.
9. Choy, J. H.; Demazeau, G.; Byeon, S. H. *J. Solid State Chem.* **1989**, *80*, 40.
10. Byeon, S. H.; Kim, I. S.; Itoh, M.; Nakamura, T. *Mat. Res. Bull.* **1993**, *28*, 597.
11. Demazeau, G.; Pouchard, M.; Thomas, M.; Colombet, J. F.; Grenier, J. C.; Fournes, L.; Soubeyroux, J. L.; Hagenmuller, P. *Mat. Res. Bull.* **1980**, *15*, 451.
12. Demazeau, G.; Byeon, S. H.; Dance, J. M.; Choy, J. H.; Pouchard, M.; Hagenmuller, P. *Eur. J. Solid State Inorg. Chem.* **1992**, *29*, 283.
13. Demazeau, G.; Pouchard, M.; Zhu, L. M.; Hagenmuller, P. *Z. Anorg. Allg. Chem.* **1987**, *555*, 64.
14. Slichter, C. P.; Drickamer, H. G. *J. Chem. Phys.* **1972**, *56*, 2142.
15. Shannon, R. D.; Prewitt, C. T. *Acta Crystallogr.* **1969**, *B25*, 925.
16. Shelwood, P. W. *Magnetochemistry*, 2nd ed.; Interscience: New York, U. S. A., 1959.
17. Buffat, B.; Demazeau, G.; Pouchard, M.; Hagenmuller, P. *Proc. Indian Acad. Sci. (Chem. Sci.)*, **1984**, *93*, 313.
18. Buffat, B.; Demazeau, G. Private communication.

## Structure Determination of D-Asparagine by Modified Pseudospectral Hartree-Fock Gradient Method

Jung-Goo Lee

HANWHA Group Research & Engineering Center, 6 Shingsung-Dong, Yousung, Taejon 305-345, Korea

Received July 12, 1994

Pseudospectral Hartree-Fock(PSHF) gradient calculations with 6-31G\*\* basis set have been carried out to determine the structure of D-Asparagine molecule ( $C_4N_2O_3H_8$ ) with improved grids and with the BFGS method. The modified PSHF method, despite partial optimization of the gradient code, turned out to be still faster than the conventional *ab initio* method, GAUSSIAN 90 program by more than twice. The optimum geometry of D-Asparagine obtained by the PSHF method is in good agreement with those calculated by the GAUSSIAN 90 program (within 0.0036 Å for bond lengths, 0.8 degrees for bond angles, and 1.6 degrees for torsional angles) except for three torsional angles. Here, rather large discrepancy of these three torsional angles (5-6 degrees) is attributed to the small differences in the optimum bond lengths and angles between the PSHF and GAUSSIAN 90 calculations.

### Introduction

As is well known, the Hartree-Fock (HF) Quantum mechanical theory has played an important role in the description of chemical and physical properties with reasonable accuracy. However, the HF calculations require large amounts of computation time as the number of basis functions(N) increases. Typically, the formal CPU time is proportional to  $N^4$ , so that it would be impractical to perform HF calculations for large molecules. Recently, Friesner's group has developed the Pseudospectral HF (PSHF) method<sup>1-6</sup> which utilizes both a physical space grid and a basis set in the evaluation of two-electron integrals and energy iterations. The PSHF method scales as  $N^3$  (in practice  $N^2$  by the use of cutoffs on local functions) rather than  $N^4$ . An order of magnitude improvements in CPU time on a 20 atom HF test case (glutamine) have been achieved<sup>6</sup> as compared to the GAUSSIAN88 computation. The Pseudospectral approach has been successfully extended<sup>7</sup> to the Generalized Valence Bond (GVB)<sup>8</sup> wave function. Also, analytic first derivatives of the HF en-

ergy has been applied in order to determine the structures of several small molecules<sup>9</sup> where both total energies and equilibrium geometries are in good agreement with those obtained from conventional *ab initio* calculations. Because of significant reduction of CPU time, the PSHF gradient method has a great potential to predict molecular structures for large compounds such as biologically important molecules and transition metal complexes. In this paper, we will report the result of the PSHF gradient computation for a medium-size molecule with an improved grid representation as an intermediate step for structure determinations of large-size molecules.

### Theoretical Overview

We briefly describe the analytical PSHF gradient method since the detailed derivation was shown in the previous paper<sup>9</sup>. The two-electron integral part ( $E_{2e}$ ) of the Hartree-Fock energy can be expressed as

$$E_{2e} = \sum_{\mu\nu} \sum_{\lambda\sigma} P_{\mu\nu} P_{\lambda\sigma} [2(\mu\nu|\lambda\sigma) - (\mu\lambda|\nu\sigma)] \quad (1)$$

where  $P$  is the density matrix given by

$$P_{\mu\nu} = \sum_{i=1}^{OCC} C_{\mu i} C_{\nu i}, \quad P_{\lambda\sigma} = \sum_{j=1}^{OCC} C_{\lambda j} C_{\sigma j} \quad (2)$$

and  $(\mu\nu|\lambda\sigma)$  is the 2-electron integrals defined by

$$(\mu\nu|\lambda\sigma) = \int_0^\infty dr_1 dr_2 \chi_\mu(1) \chi_\nu(1) \frac{1}{r_{12}} \chi_\lambda(2) \chi_\sigma(2) \quad (3)$$

The PSHF method utilizes a grid expression of  $j$ th molecular orbitals

$$\phi^{(j)}(g) = \sum_{\lambda} C_{\lambda j} \chi_{\lambda}(g) = \sum_{\lambda} R_{g,\lambda} C_{\lambda j} \quad (4)$$

and 3-center 1-electron integrals

$$A_{\lambda\sigma}(g) = \int_0^\infty dr_2 \chi_\lambda(2) \frac{1}{r_{2g}} \chi_\sigma(2) \quad (5)$$

Here,  $g$  represents a grid point in the physical space, and  $R$  is the matrix of basis functions augmented with dealiasing functions evaluated at the grid point. Since we evaluate 1-electron (3-center) integrals for the 2-electron integrals, CPU time by the PSHF method is significantly saved. Then, Eqn. (1) may be written by

$$E_{2e} = \sum_{\mu\nu} P_{\mu\nu} \sum_g [2Q_{\mu\nu}(g) \sum_{\lambda\sigma} P_{\lambda\sigma} A_{\lambda\sigma}(g) R_{\mu\nu}(g) - \sum_{\lambda} Q_{\mu\nu}(g) \sum_{\sigma} P_{\lambda\sigma} A_{\mu\sigma}(g) R_{\lambda}(g)] \quad (6)$$

where  $Q$  is the least square operator given by

$$Q = \text{Pr } S[R^+ w R]^{-1} R^+ w \quad (7)$$

In Eqn. (7),  $w$  is a diagonal matrix of grid weights,  $S$  is an overlap matrix between basis functions and basis set augmented with dealiasing set, and  $\text{Pr}$  operator projects out the dealiasing functions.

The derivative of Eqn. (1) in terms of a nuclear coordinate,  $X$  can be expressed as

$$E_{2e}^X = \frac{\partial E_{2e}}{\partial X} = \sum_{\mu\nu} \sum_{\lambda\sigma} P_{\mu\nu} P_{\lambda\sigma} \frac{\partial [2(\mu\nu|\lambda\sigma) - (\mu\lambda|\nu\sigma)]}{\partial X} \quad (8)$$

Similar to Eqn. (6), the derivative can be written in terms of grid point, *i.e.*, from Eqns. (4) and (5) and the usage of permutational symmetry of the 2-electron integrals, Eqn. (8) may be given by

$$\sum_{\mu\nu} \sum_{\lambda\sigma} P_{\mu\nu} P_{\lambda\sigma} [2(\mu^x\nu|\lambda\sigma) - (\mu^x\lambda|\nu\sigma)] = \sum_{\mu\nu} P_{\mu\nu} \sum_g [2Q_{\mu\nu}^x(g) \sum_{\lambda\sigma} P_{\lambda\sigma} A_{\lambda\sigma}(g) R_{\mu\nu}(g) - \sum_{\lambda} Q_{\mu\nu}^x(g) \sum_{\sigma} P_{\lambda\sigma} A_{\mu\sigma}(g) R_{\lambda}(g)] \quad (9)$$

where

$$Q^x = \text{Pr } S^x [R^+ w R]^{-1} R^+ w \quad (10)$$

In Eqn. (10),  $S^x$  is the analytical overlap integrals between basis set augmented with dealiasing set and first derivatives of basis functions. Again, the first derivative of 2-electron integrals is rewritten by the 1-electron (3-center) integrals

**Table 1.** Comparison of Optimized Molecular Geometries: Asparagine Bond Lengths<sup>a</sup>

Bond	PSHF(P)		GAUSSIAN 90	Error(G-P)	
	OLDGRID	NEWGRID	(G)	OLDGRID	NEWGRID
O1-C2	1.1874	1.1881	1.1885	0.0011	0.0004
C2-O6	1.3285	1.3277	1.3281	-0.0004	.0004
O6-H10	0.9486	0.9484	0.9483	-0.0003	-0.0001
C2-C3	1.5240	1.5216	1.5236	-0.0004	.0020
C3-N8	1.4408	1.4412	1.4445	.0037	.0033
N8-H11	1.0006	1.0002	1.0002	-0.0004	.0000
N8-H12	1.0010	1.0017	1.0016	.0006	-0.0001
C3-H13	1.0839	1.0835	1.0844	.0005	.0009
C3-C4	1.5301	1.5290	1.5328	-0.0003	-0.0002
C4-H14	1.0856	1.0860	1.0864	.0010	.0004
C4-H15	1.0839	1.0846	1.0846	.0007	.0000
C4-C5	1.5177	1.5169	1.5200	.0023	.0031
C5-O7	1.1990	1.1988	1.1987	-0.0003	-0.0001
C5-N9	1.3466	1.3482	1.3518	.0042	.0036
N9-H16	0.9907	0.9906	0.9907	.0000	.0001
N9-H17	0.9939	0.9937	0.9937	-0.0002	.0000

<sup>a</sup> Å units. Atom numbering Scheme is shown in Figure 1.

resulting in significant time saving.

## Computational Method

The analytic PSHF gradient method was used to optimize the geometry of a D-Asparagine molecule ( $\text{NH}_2\text{COCH}_2\text{CHNH}_2\text{COOH}$ ) with 6-31G\*\* basis set (totally 175 basis functions). Standard grids (we call these grids as OLDGRID) and dealiasing functions were used here. We have also modified atomic grids (we call these grids as NEWGRID) in the fine grids to obtain more accurate energy and geometry. Note that our grids consist of three parts, coarse, medium, and fine grids. The number of fine grids in NEWGRID is  $\sim 1300$  points per atom while that in OLDGRID is  $\sim 900$  points an atom.

We have changed the iteration Scheme in the total energy calculation. As in our previous papers, the fine grids were used only once in the SCF (Self Consistent Field) iterations. However the fine grids were used at the first iteration rather than at the latter iteration. This is because correct M. O. Coefficients obtained from the previous optimization cycle were ought to be input as an initial guess for the next cycle. Typically, the number of the SCF iterations becomes 2 to 4 iterations near and at the optimum geometry.

In the geometry optimization, we have employed the BFGS Scheme<sup>10</sup> which numerically updates force constants (Hessian). In our BFGS code, internal force constants were updated rather than Cartesian force constants. Both the BFGS and Pulay's force relaxation<sup>11</sup> (FR) methods were used for the present calculations depending on initial (FR method) or near final (BFGS method) optimizations. The optimization was terminated when all internal forces became less than 0.001 mdyn. The GAUSSIAN 90 calculations were also carried out to optimize the Asparagine molecule, and the result was compared to that obtained by the PSHF calculations. Both PSHF and GAUSSIAN 90 calculations were performed

**Table 2.** Comparison of Optimized Molecular Geometries: D-Asparagine Bond Angles and Torsional Angles<sup>a</sup>

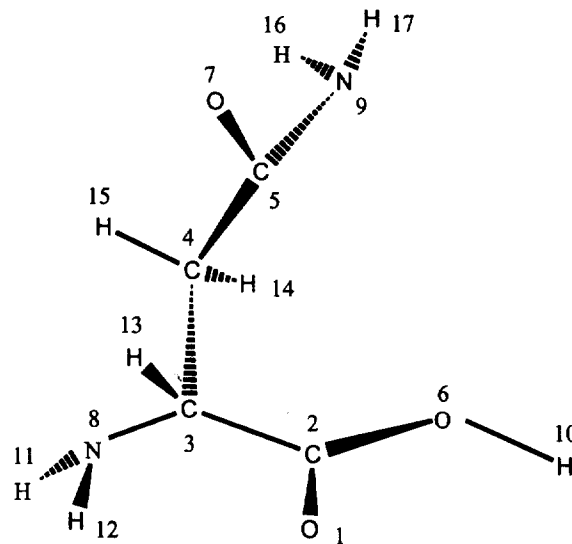
Angle	PSHF(P)		GAUSSIAN 90	Error(G-P)	
	OLDGRID	NEWGRID	(G)	OLDGRID	NEWGRID
<b>Bend</b>					
O <sub>1</sub> -C <sub>2</sub> -C <sub>3</sub>	123.9	124.2	124.6	0.7	0.4
C <sub>2</sub> -O <sub>6</sub> -H <sub>10</sub>	108.5	108.5	108.6	0.1	0.1
C <sub>6</sub> -C <sub>2</sub> -C <sub>3</sub>	113.9	113.5	113.1	-0.8	-0.4
C <sub>2</sub> -C <sub>3</sub> -N <sub>8</sub>	112.0	112.4	112.4	0.4	0.0
C <sub>3</sub> -N <sub>8</sub> -H <sub>11</sub>	110.1	110.1	110.1	0.0	0.0
C <sub>3</sub> -N <sub>8</sub> -H <sub>12</sub>	111.1	111.0	110.7	-0.4	-0.3
C <sub>2</sub> -C <sub>3</sub> -H <sub>13</sub>	105.7	105.7	106.2	0.5	0.5
C <sub>2</sub> -O <sub>3</sub> -C <sub>4</sub>	113.2	112.6	112.1	-1.1	-0.5
C <sub>3</sub> -C <sub>4</sub> -H <sub>14</sub>	111.9	111.5	111.4	-0.5	-0.1
C <sub>3</sub> -C <sub>4</sub> -H <sub>15</sub>	106.9	107.1	106.9	0.0	-0.2
C <sub>3</sub> -C <sub>4</sub> -C <sub>5</sub>	111.3	112.3	113.1	1.8	0.8
C <sub>4</sub> -C <sub>5</sub> -O <sub>7</sub>	121.4	121.8	121.9	0.5	0.1
C <sub>4</sub> -C <sub>5</sub> -N <sub>9</sub>	116.1	115.5	115.6	-0.5	0.1
C <sub>5</sub> -N <sub>9</sub> -H <sub>16</sub>	121.9	121.9	122.1	0.2	0.2
C <sub>5</sub> -N <sub>9</sub> -H <sub>17</sub>	117.7	117.7	117.6	-0.1	-0.1
<b>Torsion</b>					
O <sub>1</sub> -C <sub>2</sub> -O <sub>6</sub> -H <sub>10</sub>	-2.7	-2.5	-2.3	0.4	0.2
C <sub>3</sub> -C <sub>2</sub> -O <sub>6</sub> -H <sub>10</sub>	176.5	176.5	177.0	0.5	0.5
O <sub>1</sub> -C <sub>2</sub> -C <sub>3</sub> -N <sub>8</sub>	-22.0	-18.6	-13.4	8.6	5.2
C <sub>2</sub> -C <sub>3</sub> -N <sub>8</sub> -H <sub>11</sub>	62.3	59.0	60.2	-2.1	1.2
C <sub>2</sub> -C <sub>3</sub> -N <sub>8</sub> -H <sub>12</sub>	-55.1	-58.3	-56.7	-1.6	1.6
O <sub>1</sub> -C <sub>2</sub> -C <sub>3</sub> -H <sub>13</sub>	95.9	99.5	105.1	9.2	5.6
O <sub>1</sub> -C <sub>2</sub> -C <sub>3</sub> -C <sub>4</sub>	-148.3	-144.5	-138.7	9.6	5.8
N <sub>8</sub> -C <sub>3</sub> -C <sub>4</sub> -H <sub>14</sub>	-80.6	-79.6	-80.0	0.6	-0.4
N <sub>8</sub> -C <sub>3</sub> -C <sub>4</sub> -H <sub>15</sub>	37.1	37.6	36.9	-0.2	-0.7
N <sub>8</sub> -C <sub>3</sub> -C <sub>4</sub> -C <sub>5</sub>	153.4	154.4	153.7	0.3	-0.7
C <sub>3</sub> -C <sub>4</sub> -C <sub>5</sub> -O <sub>7</sub>	144.1	148.7	148.9	4.8	0.2
C <sub>3</sub> -C <sub>4</sub> -C <sub>5</sub> -N <sub>9</sub>	-38.6	-34.9	-35.2	-3.4	0.3
C <sub>4</sub> -C <sub>5</sub> -N <sub>9</sub> -H <sub>16</sub>	-13.4	-13.8	-13.8	0.4	0.0
C <sub>4</sub> -C <sub>5</sub> -N <sub>9</sub> -H <sub>17</sub>	-177.3	-177.7	-178.4	1.1	0.7

<sup>a</sup>Degree units. Atom numbering Scheme is shown in Figure 1.

on the Cray Y-MP supercomputer.

## Results and Discussion

Table 1 and 2 shows the internal coordinates of the D-Asparagine molecule optimized by the PSHF gradient method with the standard grids (OLDGRID) and the new grids (NEWGRID), and those obtained by the GAUSSIAN 90 program. The largest differences of the bond lengths, bond angles, and torsional angles between GAUSSIAN 90 calculations and PSHF computations with the OLDGRID are 0.0042 Å (C<sub>5</sub>-N<sub>9</sub>), 1.8 degrees (C<sub>3</sub>-C<sub>4</sub>-C<sub>5</sub>), and 9.6 degrees (O<sub>1</sub>-C<sub>2</sub>-C<sub>3</sub>-C<sub>4</sub>), respectively (atom numbers are shown in Figure 1). The bond lengths and bond angles are already in good agreement between the PSHF and GAUSSIAN 90 programs while some of the torsional angles are in poor agreement between these two results. Presumably, OLDGRID is not good enough to reproduce the geometry of D-Asparagine molecule optimized by GAUSSIAN 90, especially some torsional angles. In order

**Figure 1.** D-Asparagine.**Table 3.** Comparison of Optimized Molecular Geometries: D-Asparagine Torsional Angles<sup>a</sup>

Angle	PSHF(P)	GAUSSIAN 90	Error(G-P)
	NEWGRID	(G)	
O <sub>1</sub> -C <sub>2</sub> -O <sub>6</sub> -H <sub>10</sub>	-2.5	-2.3	0.2
C <sub>3</sub> -C <sub>2</sub> -O <sub>6</sub> -H <sub>10</sub>	177.0	177.0	0.0
O <sub>1</sub> -C <sub>2</sub> -C <sub>3</sub> -N <sub>8</sub>	-13.6	-13.4	0.2
C <sub>2</sub> -C <sub>3</sub> -N <sub>8</sub> -H <sub>11</sub>	60.5	60.2	-0.3
C <sub>2</sub> -C <sub>3</sub> -N <sub>8</sub> -H <sub>12</sub>	-56.8	-56.7	0.1
O <sub>1</sub> -C <sub>2</sub> -C <sub>3</sub> -H <sub>13</sub>	105.0	105.1	0.1
O <sub>1</sub> -C <sub>2</sub> -C <sub>3</sub> -C <sub>4</sub>	-139.0	-138.7	0.3
N <sub>8</sub> -C <sub>3</sub> -C <sub>4</sub> -H <sub>14</sub>	-80.0	-80.0	0.0
N <sub>8</sub> -C <sub>3</sub> -C <sub>4</sub> -H <sub>15</sub>	36.9	36.9	0.0
N <sub>8</sub> -C <sub>3</sub> -C <sub>4</sub> -C <sub>5</sub>	153.8	153.7	-0.1
C <sub>3</sub> -C <sub>4</sub> -C <sub>5</sub> -O <sub>7</sub>	148.5	148.9	0.4
C <sub>3</sub> -C <sub>4</sub> -C <sub>5</sub> -N <sub>9</sub>	-35.1	-35.2	-0.1
C <sub>4</sub> -C <sub>5</sub> -N <sub>9</sub> -H <sub>16</sub>	-13.8	-13.8	0.0
C <sub>4</sub> -C <sub>5</sub> -N <sub>9</sub> -H <sub>17</sub>	-178.1	-178.4	-0.3

<sup>a</sup>Degree units. Atom numbering Scheme is shown in Figure 1. Bond lengths and angles were fixed to GAUSSIAN 90 optimum geometry.

to reduce the discrepancy, we have carried out the geometry optimization by the PSHF method with NEWGRID. The optimum geometry with NEWGRID is also shown in Tables 1 and 2, the largest differences between the GAUSSIAN 90 and the PSHF methods with NEWGRID are now 0.0036 Å for C<sub>5</sub>-N<sub>9</sub> bond length, 0.8 degrees for C<sub>3</sub>-C<sub>4</sub>-C<sub>5</sub> bond angle, and 5.8 degrees for O<sub>1</sub>-C<sub>2</sub>-C<sub>3</sub>-C<sub>4</sub> torsional angle, respectively. Apparently, the PSHF optimum geometry with NEWGRID became closer to the GAUSSIAN optimum geometry. However, the Pseudospectral errors for some torsional angles (O<sub>1</sub>C<sub>2</sub>C<sub>3</sub>C<sub>4</sub>, O<sub>1</sub>C<sub>2</sub>C<sub>3</sub>H<sub>13</sub>, and O<sub>1</sub>C<sub>2</sub>C<sub>3</sub>N<sub>8</sub>) were still large (5-6 degrees). Except for these 3 torsional angles, the largest error is 1.6 degrees (C<sub>2</sub>C<sub>3</sub>N<sub>8</sub>H<sub>12</sub>). We have examined if rather large errors of these three torsional angles would come from the

**Table 4.** Total Energies and CPU Time of D-Asparagine

	Total energy (Hartrees)	CPU time <sup>a</sup> (seconds)
PSHF(P)		
OLDGRID	-489.673738	351
NEWGRID	-489.674143	447
GAUSSIAN 90(G)	-489.674202	990
Error(P-G)		
OLDGRID	-0.000464	-
NEWGRID	-0.000059	-

<sup>a</sup>CPU time for both total energy and energy gradient calculations.**Table 5.** Fine Grids for NEWGRID<sup>a</sup>

Grid for H					
Region	1	2	3	4	5
Regmx	0.400	1.173	3.200	4.765	8.000
N	4	3	5	3	4
Rlmx	0.600	4.500	8.000		
L	9	28	4		
Grid for C					
Region	1	2	3	4	5
Regmx	0.400	1.173	3.200	4.765	8.000
N	9	4	5	3	4
Rlmx	0.600	4.500	8.000		
L	9	28	3		
Grid for N					
Region	1	2	3	4	5
Regmx	0.403	1.173	3.200	4.765	8.000
N	15	3	5	3	4
Rlmx	0.200	0.600	4.500	8.000	
L	4	8	27	3	
Grid for O					
Region	1	2	3	4	5
Regmx	0.403	1.173	3.200	4.765	8.000
N	14	4	5	3	4
Rlmx	0.200	0.600	4.500	8.000	
L	4	8	28	4	

<sup>a</sup>See text for the definition of parameters.

more easily.

Table 4 shows total energies of the asparagine molecule obtained by the GAUSSIAN 90 program and by the PSHF gradient program with both OLDGRID and NEWGRID. The PSHF energy with NEWGRID turned out to be slightly better than that with OLDGRID although the latter energy is already close to the GAUSSIAN 90 energy.

The CPU time for one optimization cycle is also listed in Table 4. Despite the fact that the current code is suboptimal, the PSHF gradient calculation with NEWGRID is still faster than the GAUSSIAN 90 computation by more than twice. The PSHF method with OLDGRID may be inferior in prediction of optimum geometries to that with NEWGRID. However, it can be used to calculate intermediate geometries and force constants with less CPU time. Therefore, the PSHF gradient method with the use of both OLDGRID and NEWGRID will save the CPU time significantly during entire geometry optimization cycles compared to conventional implementations.

The details of fine grids for NEWGRID is listed in Table 5. Here, Regmx(*i*) is the outer boundary (in bohr, measured from nucleus) of radial region *i*, *N*(*i*) the number of radial shells to be used in the radial region *i*, Rlmx(*j*) the outer boundary for radial region *j* (but different from Regmx), and *L*(*j*) sets the number of grid points on the radial region *j*. The grid points (discovered by Lebedev) have octahedral symmetry and range in size up to 302 points<sup>6</sup>. Compared to OLDGRID, NEWGRID has two main differences, (i) more grid points (larger *L*) are included in bonding region (0.6-4.5 bohr) and (ii) *N*(1) of C atom is increased from 4 to 9 radial shells. It is generally true to use more grid points in order to obtain accurate molecular geometries, but more balanced grid selection is also necessary.

## Conclusion

We have shown that the PSHF method is capable of yielding equilibrium geometry and total energy for a medium-size molecule, D-Asparagine with use of new grids and with more standardized option such as updating force constants. However, determination of some torsional angles turned out to be rather difficult because they are very sensitive to small differences of the optimum bond lengths and angles between the PSHF and GAUSSIAN 90 methods. We also showed significant time saving in geometry optimizations by the use of PSHF gradient method compared to GAUSSIAN 90 program. More work will be done to improve both accuracy and speed in geometry optimization Scheme by elaborating grids and dealiasing functions, and by optimizing the gradient code.

**Acknowledgment.** The author would like to thank Professor Richard A. Friesner at Columbia University for his useful suggestions. The PSHF and GAUSSIAN 90 calculations were carried out at the Pittsburgh supercomputing center.

## References

1. Friesner, R. A. *Chem. Phys. Lett.* **1985**, *116*, 39.
2. Friesner, R. A. *J. Chem. Phys.* **1986**, *85*, 1462.
3. Friesner, R. A. *J. Chem. Phys.* **1987**, *86*, 3522.

small differences of bond lengths and angles. In order to test this assumption, we optimized these three torsional angles by the PSHF method with NEWGRID while we kept the other 42 internal coordinates fixed to the corresponding optimum GAUSSIAN 90 coordinates. All these three optimized torsional angles agreed to the corresponding GAUSSIAN 90 geometries within 0.3 degrees. Furthermore, we optimized all 14 torsional angles with all the bond lengths and angles fixed to the corresponding GAUSSIAN 90 internal coordinates. Again, the Pseudospectral error of 14 torsional angles turned out to be very small, at most 0.4 degrees as shown in Table 3. This suggests that small differences in bond lengths and angles do cause rather large errors in the torsional angles because of the small torsional force constants. The calculated equilibrium geometry of D-Asparagine molecule should help experimentalists identify the structure

- Friesner, R. A. *J. Phys. Chem.* **1988**, *92*, 3091.
- Ringnalda, M. N.; Won, Y.; Friesner, R. A. *J. Chem. Phys.* **1990**, *92*, 1163.
- Ringnalda, M. N.; Belhadj, M.; Friesner, R. A. *J. Chem. Phys.* **1990**, *93*, 3397.
- Langlois, J. M.; Muller, R. P.; Coley, T. R.; Goddard, W. A. III; Ringnalda, M. N.; Won, Y.; Friesner, R. A. *J. Chem. Phys.* **1990**, *92*, 7488.
- Bobrowicz, F. W.; Goddard, W. A. III in *Modern Theoretical Chemistry: Methods of Electronic Structure Theory*; Schaefer, H. F. III, Ed.: Plenum; New York, **1977**, *3*, 79.
- Won, Y.; Lee, J.-G.; Ringnalda, M. N.; Friesner, R. A. *J. Chem. Phys.* **1991**, *94*, 8152.
- Somons, J.; Jorgensen, P.; Taylor, H.; Ozment, J. *J. Phys. Chem.* **1984**, *87*, 2475.
- Pulay, P. in *Modern Theoretical Chemistry: Applications of Electronic Structure Theory*; Schaefer, H. F. III, Ed.; Plenum, New York, **1977**, *4*, 153.

## Shape Selective Oxygen Transfer to Olefins Catalyzed by Sterically Hindered Iron Porphyrins

Kwang-Hyun Ahn and John T. Groves\*

Department of Chemistry, College of Natural Science,  
Kyung Hee University, Yongin-Kun, Kyung Ki-Do, 449-701, Korea

\*Department of Chemistry, Princeton University, Princeton, New Jersey 08544, U. S. A.

Received July 13, 1994

Epoxidation of olefins catalyzed by iron-tetraarylporphyrins were studied to see the shape selectivity in the competing reaction between *cis*- and *trans*- or internal and external olefins. *Cis*-olefins were more reactive than *trans*-olefins in the competing reaction between *cis*- and *trans*-olefins. Interestingly, in the epoxidation of *cis*- $\beta$ -methylstyrene by  $\alpha\beta\alpha\beta$  atropisomer of Fe(III)TNPPPCl and iodosylbenzene, 27% of total product was phenylacetone. The unusually large amount of phenylacetone may be produced by hydride rearrangement of carbocationic intermediate. Regioselectivity of the reaction was also studied by using the most sterically hindered Fe(III)TTPPPCl. In the epoxidation of limonene with Fe(III)TTPPPCl, the disubstituted double bond was more reactive than trisubstituted double bond. This is in contrast to the results obtained with other iron-tetraarylporphyrins. Similar trend was also observed in the competing reaction between mono- and di-substituted olefins.

### Introduction

Epoxidation of olefins catalyzed by metal complex has been extensively studied recently because of the versatility of epoxides as useful intermediates in the organic synthesis.<sup>1</sup> Stereo- and regioselective transformation of olefins by discriminating the substrates based on size and shape typical of enzymatic reaction are one of the main objects in the reaction. For example, a chiral epoxide can be obtained by optimizing the steric and electronic effect of a metal ligand.<sup>2</sup> The substrates for high enantioselectivities in the epoxidations are, however, limited to only olefins with certain functional groups such as allylic alcohol.

Metalloporphyrins have been used as effective catalysts for the oxidation of hydrocarbons with various oxidants in analogy to cytochrome P-450 catalyzed epoxidation reactions.<sup>3</sup> Shape selective oxygenations of hydrocarbons were attempted in some cases to mimic the enzyme.<sup>4</sup> High valent metal-oxo complexes have been usually proposed as an active oxidant in the reaction.

Iron porphyrins catalyze the oxygen transfer from iodosylbenzene to olefins.<sup>5</sup> Epoxides are produced as a major product in the reaction along with some other compounds such

as allylic alcohols, aldehydes and ketones. The active oxidant is believed to be an oxo-iron(IV) porphyrin cation radical complex analogous to compound I of horse radish peroxidase.<sup>6</sup> A great deal of work has been reported regarding the mechanism of the oxygen atom transfer from the oxo-iron complex to olefins.<sup>7</sup> Substrate selectivities observed in the epoxidation reaction often contribute to the elucidation of the mechanism.

It has been reported that olefins under different steric and electronic environments give different reactivities in the iron porphyrin catalyzed epoxidation.<sup>5b</sup> The reactivity difference of olefins under given conditions are known to be dependent upon the structure of iron porphyrins.

We report here the shape selective epoxidation of olefins catalyzed by sterically hindered iron porphyrins such as  $\alpha\beta\alpha\beta$  isomer of chloro[5,10,15,20-tetra[*o*-(*p*-nitrophenyl)phenyl]porphyrinato] iron(III) [Fe(III)TNPPPCl] (Figure 1) and chloro[5,10,15,20-tetra[2,4,6-triphenylphenyl]porphyrinato] iron(III) [Fe(III)TTPPPCl] (Figure 2). We have found that a large amount of phenylacetone was unexpectedly produced in the epoxidation of *cis*- $\beta$ -methylstyrene catalyzed by  $\alpha\beta\alpha\beta$  Fe(III)TNPPPCl, which might give a clue for the mechanism of iron-porphyrin catalyzed epoxidation.